

Out-of-plane intensity modulation of spin susceptibility in $\text{Ba}_{0.75}\text{K}_{0.25}\text{Fe}_2\text{As}_2$ as seen via time-of-flight neutron spectroscopy

Naoki Murai,^{1,*} Katsuhiko Suzuki,^{2,†} Masamichi Nakajima,³ Maiko Kofu,¹
Seiko Ohira-Kawamura,¹ Yasuhiro Inamura,¹ and Ryoichi Kajimoto¹

¹*Materials and Life Science Division, J-PARC Center, Japan Atomic Energy Agency, Tokai, Ibaraki 319-1195, Japan*

²*Department of Mechanical Engineering, National Institute of Technology,
Niihama College, Niihama 792-8580, Japan*

³*RIKEN Center for Emergent Matter Science (CEMS), Wako 351-0198, Japan*

(Dated: December 24, 2024)

We present a time-of-flight inelastic neutron scattering study of the iron-based superconductor $\text{Ba}_{0.75}\text{K}_{0.25}\text{Fe}_2\text{As}_2$, focusing on its spin dynamics. Our measurements reveal a periodic intensity modulation of magnetic signals along the out-of-plane direction, which deviates from the behavior typically expected for two-dimensional magnetic materials. Using an effective model derived from density functional theory calculations, we demonstrate that the observed out-of-plane modulated spin susceptibility originates from the intrinsic three-dimensionality of the electronic band structure. Our study reveals the limitations of the widely assumed two-dimensional nature of spin susceptibility in iron-based superconductors, highlighting the importance of incorporating three-dimensional aspects of the electronic band structure for accurate modeling of spin dynamics.

I. Introduction

The discovery of iron-based superconductors (FeSCs) in 2008[1] generated considerable interest in the condensed matter physics community. Since then, extensive research efforts have been directed toward uncovering the mechanisms behind high- T_c superconductivity[2–7]. In most FeSCs, superconductivity emerges in close proximity to an antiferromagnetic (AFM) phase, indicating the potential role of spin fluctuations in the pairing mechanism. The study of such an unconventional pairing, mediated by spin fluctuations, has a long history dating back to the seminal works on heavy fermion materials[8, 9] and later on the cuprates[10]. The discovery of FeSCs renewed this research interest in the community, and within a few years, the consensus converged around the spin-fluctuation-mediated pairing scenario[11–18]. Today, FeSCs are considered prototypical model systems—alongside heavy fermion materials and cuprates—in which magnetism plays a fundamental role in the pairing mechanism[19].

In FeSCs, the low-energy bands near the Fermi level are primarily derived from Fe $3d$ orbitals, which form multiple hole and electron Fermi surfaces. Thus, constructing a multi-orbital model that includes all five Fe $3d$ orbitals is an essential first step in theoretical treatment. The increasing sophistication of electronic structure theory has greatly facilitated the derivation of material-specific model Hamiltonians based on density functional theory (DFT)[20–22]. Through their extensive application in FeSC research, these first-principles techniques have matured into a well-established theoretical framework, enabling accurate predictions of magnetic instability in the stripe-type AFM channel[11–18, 23–26], con-

sistent with neutron scattering experiments[27–75].

Despite this success, several issues remain to be addressed. One important but often overlooked aspect is the three-dimensional (3D) nature of the magnetism. Underdoped FeSCs exhibit long-range 3D magnetic ordering below the Néel temperature (T_N). Consequently, the paramagnetic spin susceptibility, which reflects a tendency towards a magnetic phase transition, is expected to peak at a characteristic position in the 3D momentum space, corresponding to the ground state ordering wavevector. However, previous theoretical analyses have often determined the magnetic wavevector solely from the peak position of the in-plane spin susceptibility, implicitly assuming its two-dimensional (2D) nature without accounting for the out-of-plane momentum[54, 70]. Therefore, it is essential to rigorously test whether the theoretical model can accurately capture the 3D nature of spin susceptibility beyond the 2D assumption.

The present study addresses this issue by comparing neutron scattering data with calculations of the full 3D spin susceptibility, including the out-of-plane direction. Through time-of-flight (TOF) neutron spectroscopy on the prototypical 122 type FeSC $\text{Ba}_{0.75}\text{K}_{0.25}\text{Fe}_2\text{As}_2$, we observed a non-uniform intensity distribution of magnetic scattering along the out-of-plane $(0.5, 0.5, L)$ direction. Unlike purely 2D systems, the magnetic signals are enhanced at odd L positions, highlighting the 3D aspect of the spin susceptibility. Using a first-principles model that fully incorporates the 3D electronic structure, we successfully reproduce the experimentally observed out-of-plane intensity modulation. The agreement between theoretical and experimental results underscores the necessity of incorporating the three-dimensionality of the electronic band structure, beyond a simplified 2D treatment, for accurately describing the magnetic excitation spectra of FeSCs.

* naoki.murai@j-parc.jp

† Ka.Suzuki@niihama.kosen-ac.jp

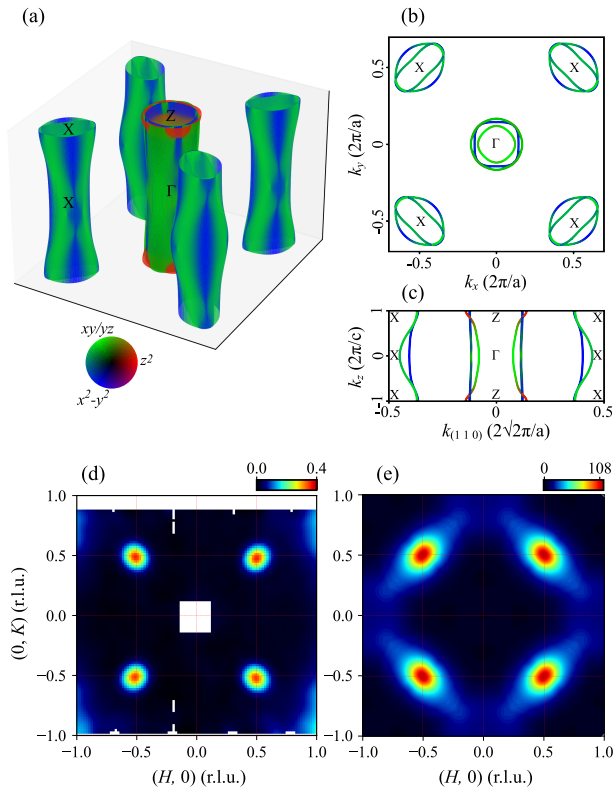


FIG. 1. (a)-(c) 3D and cross-sectional views of the Fermi surface for BaFe_2As_2 , with the Fermi level shifted to account for 25% K-doping. Panel (a) shows a 3D view, (b) a top view from the $(0\ 0\ 1)$ direction, and (c) a side view from the $(1\ \bar{1}\ 0)$ direction. The color code represents the orbital character projected onto the Fermi surface. Panels (d) and (e) show the experimental and theoretical spin susceptibilities at $\omega = 10$ meV, respectively. The measurements were performed with an incident neutron energy of $E_i = 31.3$ meV at $T = 30$ K. Note that panels (d) and (e) use different intensity scales in arbitrary units and cannot be directly compared.

II. Experimental methods

Single crystals of $\text{Ba}_{0.75}\text{K}_{0.25}\text{Fe}_2\text{As}_2$ were grown using the FeAs-flux method[70, 76]. At room temperature, this material crystallizes in a body-centered tetragonal structure ($I4/mmm$) with lattice constants of $a = b = 3.935$ Å and $c = 13.135$ Å. Upon cooling, a magnetic transition occurs at $T_N = 95$ K.

Inelastic neutron scattering (INS) measurements were performed using the 4SEASONS[77, 78] and AMATERAS[79] TOF chopper spectrometers at the Materials and Life Science Experimental Facility of J-PARC. For the 4SEASONS measurements, an incident neutron energy (E_i) of 31.3 meV was primarily used, with an energy resolution of 1.5 meV at the elastic position. An array of co-aligned single crystals with a total mass of 5.0 g was mounted on a top-loading cryostat, with the tetragonal $(H, 0, L)$ scattering plane oriented horizon-

tally. During data collection, the angle ϕ between the incident neutron beam and the c -axis of the crystal was fixed at $\phi = 0$. For the AMATERAS measurements, we used E_i values of 7.74 and 15.15 meV, with corresponding energy resolutions of 0.25 and 0.56 meV, respectively. The same array of co-aligned crystals was mounted on a bottom-loading cryostat, with the tetragonal (H, H, L) scattering plane oriented horizontally. The sample was rotated over a range of $\phi \in [-40^\circ, +40^\circ]$ around the vertical axis, with data collected at 1° increments. The neutron event data were processed to extract the wavevector- and energy-dependent scattering function $S(\mathbf{Q}, \omega)$ using the UTSUSEMI and D4MAT2 software packages[80, 81]. Unless specified otherwise, the momentum transfer \mathbf{Q} is expressed in terms of the tetragonal unit cell as $\mathbf{Q} = H\mathbf{a}^* + K\mathbf{b}^* + L\mathbf{c}^* \equiv (H, K, L)$ in reciprocal lattice units (r.l.u.).

III. Theoretical methods

The unit cell of BaFe_2As_2 contains two Fe atoms due to the presence of two inequivalent As positions, requiring a ten-orbital model for an accurate description of the electronic band structure. However, since the magnetic moment is localized on the Fe atoms, the INS signals reflect the symmetry of the unfolded Brillouin zone (BZ) for the Fe sublattice (1-Fe/unit cell), rather than that of the crystallographic unit cell (2-Fe/unit cell)[25, 45]. Consequently, a five-orbital model in the 1-Fe/unit cell BZ provides a more appropriate starting point for describing spin susceptibility in the paramagnetic phase. With this in mind, we constructed an effective five-orbital tight-binding model of BaFe_2As_2 by unfolding the ten-orbital model into an effective 1-Fe/unit cell BZ[18]. To obtain the tight-binding model from first principles, we used the QUANTUM ESPRESSO[82, 83] and WANNIER90[84, 85] software packages. The DFT calculations were performed using the generalized gradient approximation (GGA) exchange-correlation functional[86] with a cutoff energy of 40 Ry and a k -point mesh of $8 \times 8 \times 8$. The K substitution effect in $\text{Ba}_{0.75}\text{K}_{0.25}\text{Fe}_2\text{As}_2$ was modeled as a rigid shift of the Fermi level. To account for the experimentally observed band narrowing due to electron correlations, we rescaled the DFT band structure by a factor of three to match the angle-resolved photoemission spectroscopy (ARPES) data[70, 87]. The dynamical spin susceptibility was then obtained using the random phase approximation (RPA):

$$\hat{\chi}_s(\mathbf{q}, \omega) = \hat{\chi}_0(\mathbf{q}, \omega) [\hat{I} - \hat{S} \hat{\chi}_0(\mathbf{q}, \omega)]^{-1}, \quad (1)$$

where \hat{S} is the interaction vertex matrix[88]. The irreducible susceptibility $\hat{\chi}_0(\mathbf{q}, \omega)$ is given as

$$\begin{aligned} \hat{\chi}_0^{l_1, l_2, l_3, l_4}(\mathbf{q}, \omega) &= \sum_{\mathbf{k}} \sum_{n, m} \frac{f(\varepsilon_{\mathbf{k}+\mathbf{q}}^n) - f(\varepsilon_{\mathbf{k}}^m)}{\omega - \varepsilon_{\mathbf{k}+\mathbf{q}}^n + \varepsilon_{\mathbf{k}}^m + i\delta} \\ &\times U_{l_1, n}(\mathbf{k} + \mathbf{q}) U_{l_4, m}(\mathbf{k}) U_{m, l_2}^\dagger(\mathbf{k}) U_{n, l_3}^\dagger(\mathbf{k} + \mathbf{q}), \end{aligned} \quad (2)$$

where f , $\varepsilon_{\mathbf{k}}^m$, and $U_{l,m}(\mathbf{k})$ represent the Fermi distribution function, the eigenvalue of the Bloch state with momentum \mathbf{k} and band index m , and the matrix element of the unitary transformation that connects the orbital and band spaces, respectively. The orbital index $l \in (1, \dots, 5)$ corresponds to the Fe 3d orbitals ($d_{xy}, d_{xz}, d_{yz}, d_{x^2-y^2}, d_{z^2}$). As the elements of \hat{S} , we consider the Hubbard-type interactions, *i.e.*, intra- and inter-orbital onsite interaction U , U' , Hund's coupling J , and pair hopping J' . The calculation was performed on a k -point mesh of $128 \times 128 \times 128$ with $U = 0.41$ eV, $U' = U - 2J$, $J = J' = U/8$, temperature of $k_B T = 3.0 \times 10^{-2}$ eV, and smearing factor of $\delta = 5.0 \times 10^{-3}$ eV.

IV. Results and discussion

We begin this section with a brief overview of the magnetic instability inherent in the Fermi surface geometry of FeSCs. Figures 1(a)-(c) display the orbital-resolved Fermi surface for 25% K-doped BaFe₂As₂ [89]. The Fermi surface consists of hole pockets at the Brillouin zone center (Γ) and electron pockets at the zone corner (X). The presence of the well-nested hole and electron pockets leads to the reasonable expectation of an enhanced spin susceptibility at the nesting wavevector $\mathbf{q} = (0.5, 0.5)$, connecting Γ to X . This expectation is confirmed by calculating the spin susceptibility within RPA, which reveals a prominent peak at this wavevector, consistent with INS experiments [see Figs. 1(d) and (e)].

Extensive research to date has primarily focused on observing magnetic excitation spectra within the 2D (H, K) plane, with limited focus given to their 3D structure along the out-of-plane ($0.5, 0.5, L$) direction. This limited focus stems from the prevailing assumption that the spin susceptibility of FeSCs is largely independent of L , reflecting their quasi-2D electronic structure. Consequently, earlier INS studies on FeSCs often employed a fixed-geometry scan suitable for 2D materials, in which $S(\mathbf{Q}, \omega)$ is obtained by projecting the observed signal onto the (H, K, E) coordinate system while assuming its negligible L -dependence. Meanwhile, ARPES studies reveal that the shape and orbital character of the Fermi surface depend on the out-of-plane momentum k_z [90–97], indicating a subtle yet non-negligible three-dimensionality in the electronic structure. This 3D aspect is further supported by the calculated Fermi surface in Fig. 1(c), showing its warping along the k_z direction. Considering the strong sensitivity of spin susceptibility to the electronic structure, it becomes crucial to explore how this 3D electronic structure influences the out-of-plane spin susceptibility.

To address this, we performed measurements of the full four-dimensional (4D) $S(\mathbf{Q}, \omega)$ by combining large datasets collected from multiple crystal orientations. Unlike fixed-geometry scans, which cover only a sparse set of hypersurfaces in the 4D (\mathbf{Q}, ω)-space, this multi-orientation approach substantially expands the accessible region, thereby enabling comprehensive measurement of the full 4D volume [98, 99]. As a demonstration, we gen-

erated a 3D density map of the magnetic signal in the (H, K, L) space at $\omega = 5 \pm 2$ meV [Fig. 2(a)]. The magnetic signal centered at $(0.5, 0.5)$ extends in a rod-like pattern along the L direction, as expected for a quasi-2D system. However, the intensity distribution varies significantly with L . To better visualize these variations, we sliced the 3D density map along the 2D (H, H, L) plane [Fig. 2(b)]. The magnetic signal is enhanced at odd L positions and suppressed at even L positions, leading to periodic intensity modulation along the L direction. The observed intensity distribution deviates from the expectation for purely 2D magnetic systems. The L -modulated intensity distribution is also evident in the energy spectrum along the $(0.5, 0.5, L)$ direction

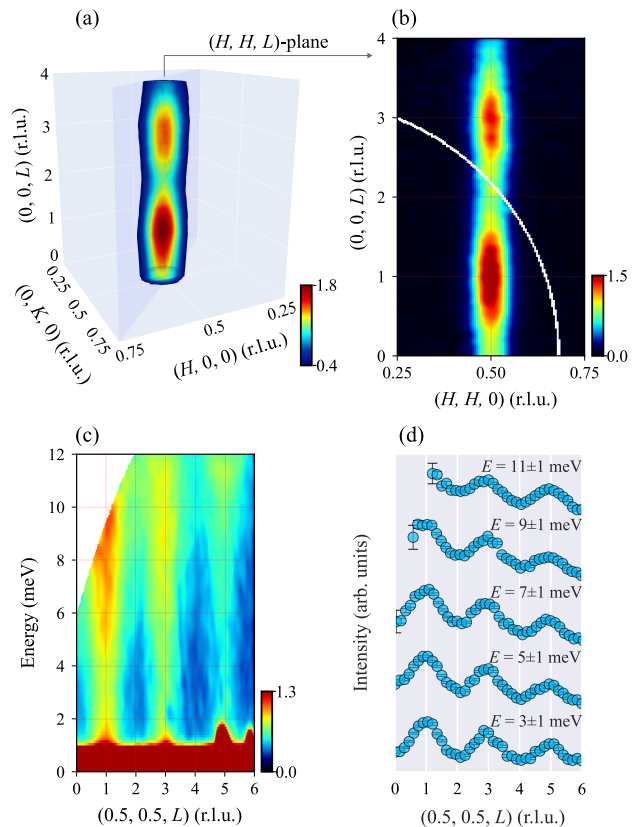


FIG. 2. (a) A 3D density map of magnetic scattering intensity in the (H, K, L) space, averaged over the energy range $\omega = 5 \pm 2$ meV. To enable clear visualization of the intensity distribution throughout the 3D volume, different isosurfaces were rendered partially transparent. (b) A horizontal slice of the 3D density map in panel (a), visualizing the intensity distribution in the 2D (H, H, L) plane. Intensities along the ($\bar{H}, H, 0$) direction were integrated over a range of ± 0.02 r.l.u. (c) Energy dependence of the magnetic scattering along the $(0.5, 0.5, L)$ direction, with integration ranges of $|H - 0.5| < 0.05$ r.l.u. and $|K - 0.5| < 0.05$ r.l.u. (d) Constant energy plots along the $(0.5, 0.5, L)$ direction for various energy transfers, with curves vertically shifted for clarity. All data were collected using an incident neutron energy of $E_i = 15.15$ meV at $T = 35$ K.

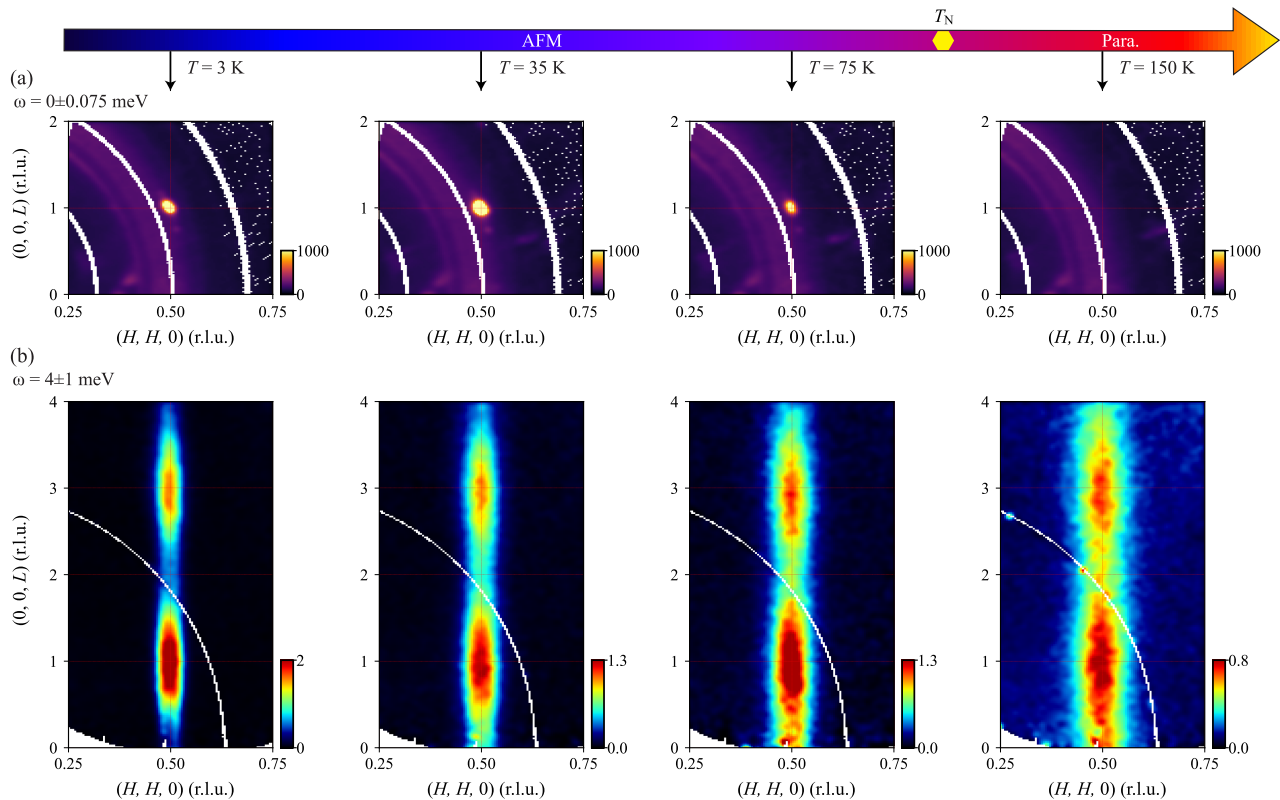


FIG. 3. Temperature dependence of magnetic scattering in the (H, H, L) plane at (a) $\omega = 0 \pm 0.075$ meV and (b) $\omega = 3 \pm 1$ meV. At finite energy transfer in panel (b), the magnetic scattering shows a momentum dependence with peaks at odd L positions. These peaks persist even above T_N , indicating robust out-of-plane AFM correlations. The measurements were performed using an incident neutron energy of $E_i = 7.74$ meV. To construct the constant energy maps in (a) and (b), the data along the $(\bar{H}, H, 0)$ direction were integrated over ranges of ± 0.02 r.l.u. and ± 0.035 r.l.u., respectively.

[Fig. 2(c)] and becomes even clearer when taking constant energy slices along this direction [Fig. 2(d)]. Similar L -dependent intensity modulation has also been reported in other 122 systems, including BaFe_2As_2 [37, 43, 45, 47, 75], SrFe_2As_2 [31, 72] and CaFe_2As_2 [32, 69].

Figure 3 shows the temperature dependence of the magnetic scattering in the (H, H, L) plane. As shown in Fig. 3(a), the magnetic Bragg peak at the odd L position disappears once the temperature exceeds T_N . At finite energy transfer $\omega = 4 \pm 1$ meV [Fig. 3(b)], the magnetic signal also peaks at odd L positions, similar to the magnetic Bragg peak; however, its L -modulated momentum dependence persists even above T_N . Similarly, the L -dependent magnetic signal has been reported to persist against doping-induced suppression of the AFM order[45, 47, 75]. Thus, regardless of whether the AFM order is suppressed by temperature or doping, the out-of-plane magnetic signal remains peaked at odd L positions. This behavior is consistent with the expectation that the paramagnetic spin susceptibility—a direct measure of the magnetic ordering tendency—should peak at the AFM wavevector $\mathbf{q} = (0.5, 0.5, 1)$, rather than exhibit a purely

2D intensity profile along the L direction. Using the first-principles model, we reproduce the in-plane spin susceptibility peaking at $\mathbf{q} = (0.5, 0.5)$ [see Fig. 1(e)]. However, whether the same calculations accurately capture the L -modulated spin susceptibility reflecting the out-of-plane AFM instability remains open for further theoretical investigation.

To address this question, we computed the out-of-plane spin susceptibility using RPA. To fully account for the explicit L dependence, we considered the full 3D momentum dependence of the electronic band structure. Figure 4(a) shows the calculated spin susceptibility at $E = 10$ meV on the (H, H, L) plane. Consistent with the experimental data, we observe a non-uniform intensity distribution along the $(0.5, 0.5, L)$ direction, with maxima at odd L and minima at even L positions. The energy spectrum in Fig. 4(b) further confirms the presence of the L -dependent intensity modulation. To clarify the orbitally resolved contributions to the spin susceptibility, we show the intraorbital components ($l_1 = l_2 = l_3 = l_4$) in Fig. 4(c). For all orbitals, momentum dependence is similar, peaking at $L = 1$; however, the overall inten-

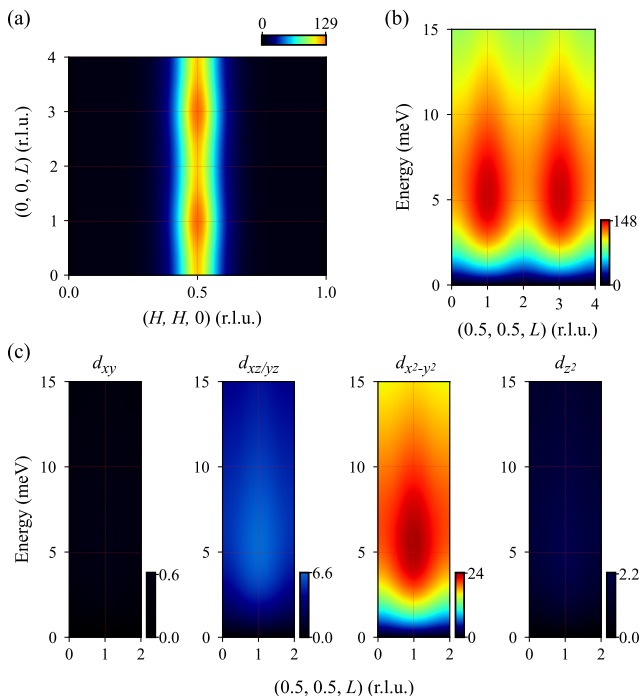


FIG. 4. (a) Constant-energy map of the RPA spin susceptibility at $\omega = 10$ meV, plotted in the (H, H, L) plane. (b) Energy dependence of the RPA spin susceptibility along the out-of-plane $(0.5, 0.5, L)$ direction. The spin susceptibility is enhanced at $L = 1$, in agreement with the experimental data. (c) Comparison of the orbital-resolved components of the spin susceptibility.

sity varies significantly across orbitals. The $d_{xz/yz}$ and $d_{x^2-y^2}$ orbital-derived components exhibit strong intensity, highlighting these as dominant orbital characters near the Fermi level.

Thus, starting from a realistic multi-orbital model based on first-principles band structure calculations, we can reproduce the L -modulated spin excitation spectrum. As shown in Eq. (2), the (\mathbf{q}, ω) -dependence of the dynamical spin susceptibility is directly related to the electronic band structure. In an ideal 2D system without k_z dispersion, no intensity modulation in spin susceptibility is expected along L . The observed L -modulation therefore reflects the k_z -dependent electronic band structure of 122 systems, as incorporated through DFT calculations. In addition, the calculated paramagnetic spin susceptibility, which peaks at $\mathbf{q} = (0.5, 0.5, 1)$, is consistent with the experimentally observed out-of-plane AFM structure, thus demonstrating the effectiveness of our combined DFT and RPA approach in identifying the leading magnetic instability of FeSCs.

Since spin susceptibility also stems from electronic states away from the Fermi level, the conventional nesting picture, which relies solely on the Fermi surface geometry, often fails to identify the magnetic ordering wavevector. Indeed, previous ARPES work has shown that

shifting the hole Fermi surfaces by the AFM wavevector $\mathbf{q} = (0.5, 0.5, 1)$ does not perfectly overlap with the electron Fermi surfaces[92]. To verify this observation, we isolated the contributions of the Fermi surface geometry to the spin susceptibility by evaluating Eq. (2) using only eigenvalues close to the Fermi level. The peak of the resulting susceptibility at $L = 1$ became notably less pronounced than when contributions from all energies were included. Thus, much of the spin susceptibility arises from states away from the Fermi level, and therefore, visually inspecting the Fermi surface geometry alone is insufficient for accurately identifying the magnetic wavevector[92]. Instead, a detailed calculation of the spin susceptibility using a realistic model is required to capture the correct magnetic intensity distribution in the (\mathbf{q}, ω) -space.

Our discussion concludes with a possible direction for future research. As evidenced by the agreement between the experimental and theoretical spin susceptibility, standard DFT calculations provide a reasonable starting point for modeling the electronic structure of the 122 system. However, in more strongly correlated FeSCs like FeSe, deviations from DFT calculations become increasingly evident[100, 101]. To address the limitations of standard DFT, more advanced approaches—such as DFT+U[102, 103], hybrid functional calculations[102], dynamical mean field theory (DMFT)[104, 105], and quasiparticle self-consistent GW theory (QS GW)[106]—are required. In this context, we note a recent INS study on FeSe that revealed ferromagnetic (FM) spin correlations along the out-of-plane direction[107]. Such behavior has been observed only in FeSe among FeSCs, making it a unique case for exploring possible connections to strong electron correlations. A promising future direction is to investigate whether standard DFT is sufficient to capture the out-of-plane FM spin susceptibility in FeSe, or whether beyond-DFT methods are necessary. Systematic validation of theoretical models against experimental data is essential, particularly in the study of unconventional superconductors. These efforts will strengthen the predictive power of theoretical approaches and provide deeper insights into the unconventional pairing mechanism in FeSCs.

V. Summary

Since FeSCs are often considered quasi-2D magnetic materials, their spin susceptibility along the out-of-plane direction has attracted relatively little attention. This study examined the validity of the 2D assumption of spin susceptibility by analyzing the full 3D momentum-space structure. Using TOF neutron spectroscopy on the prototypical 122 material $\text{Ba}_{0.75}\text{K}_{0.25}\text{Fe}_2\text{As}_2$, we observed a non-uniform magnetic signal along the out-of-plane $(0.5, 0.5, L)$ direction, with peaks at odd L positions and minima at even L positions. To understand the origin of this deviation from strictly 2D behavior, we constructed an effective first-principles model that fully incorporates the 3D electronic band structure. Apply-

ing RPA to this model, we reproduced the L -dependent intensity modulation observed in neutron scattering results. Our theoretical analysis highlights the essential role of the 3D electronic band structure in shaping the magnetic excitation spectrum of FeSCs, particularly its out-of-plane structure. This work provides a benchmark for theoretical approaches based on first-principles models, showcasing their predictive power in identifying the

magnetic instabilities in FeSCs.

VI. Acknowledgments

This research was supported by the Japan Society for the Promotion of Science through the Grant-in-Aid for Young Scientists (Grant Nos. 18K13500 and 19K14666). Neutron scattering experiments were performed at the Materials and Life Science Experimental Facility of J-PARC under Proposal Nos. 2021I0014 and 2019I0001.

-
- [1] Y. Kamihara, T. Watanabe, M. Hirano, and H. Hosono, *J. Am. Chem. Soc.* **130**, 3296 (2008).
- [2] K. Ishida, Y. Nakai, and H. Hosono, *J. Phys. Soc. Jpn.* **78**, 062001 (2009).
- [3] J. Paglione and R. L. Greene, *Nat. Phys.* **6**, 645 (2010).
- [4] P. J. Hirschfeld, M. M. Korshunov, and I. I. Mazin, *Rep. Prog. Phys.* **74**, 124508 (2011).
- [5] A. Chubukov and P. J. Hirschfeld, *Phys. Today* **68**, 46 (2015).
- [6] P. J. Hirschfeld, *C. R. Phys.* **17**, 197 (2016).
- [7] R. M. Fernandes, A. I. Coldea, H. Ding, I. R. Fisher, P. J. Hirschfeld, and G. Kotliar, *Nature* **601**, 35 (2022).
- [8] K. Miyake, S. Schmitt-Rink, and C. M. Varma, *Phys. Rev. B* **34**, 6554 (1986).
- [9] D. J. Scalapino, E. Loh, and J. E. Hirsch, *Phys. Rev. B* **34**, 8190 (1986).
- [10] P. Monthoux, A. V. Balatsky, and D. Pines, *Phys. Rev. Lett.* **67**, 3448 (1991).
- [11] I. I. Mazin, D. J. Singh, M. D. Johannes, and M. H. Du, *Phys. Rev. Lett.* **101**, 057003 (2008).
- [12] K. Kuroki, S. Onari, R. Arita, H. Usui, Y. Tanaka, H. Kontani, and H. Aoki, *Phys. Rev. Lett.* **101**, 087004 (2008).
- [13] K. Kuroki, H. Usui, S. Onari, R. Arita, and H. Aoki, *Phys. Rev. B* **79**, 224511 (2009).
- [14] S. Graser, T. A. Maier, P. J. Hirschfeld, and D. J. Scalapino, *New J. Phys.* **11**, 025016 (2009).
- [15] S. Graser, A. F. Kemper, T. A. Maier, H.-P. Cheng, P. J. Hirschfeld, and D. J. Scalapino, *Phys. Rev. B* **81**, 214503 (2010).
- [16] H. Ikeda, R. Arita, and J. Kuneš, *Phys. Rev. B* **81**, 054502 (2010).
- [17] K. Suzuki, H. Usui, and K. Kuroki, *J. Phys. Soc. Jpn.* **80**, 013710 (2011).
- [18] K. Suzuki, H. Usui, and K. Kuroki, *Phys. Rev. B* **84**, 144514 (2011).
- [19] D. J. Scalapino, *Rev. Mod. Phys.* **84**, 1383 (2012).
- [20] N. Marzari and D. Vanderbilt, *Phys. Rev. B* **56**, 12847 (1997).
- [21] I. Souza, N. Marzari, and D. Vanderbilt, *Phys. Rev. B* **65**, 035109 (2001).
- [22] N. Marzari, A. A. Mostofi, J. R. Yates, I. Souza, and D. Vanderbilt, *Rev. Mod. Phys.* **84**, 1419 (2012).
- [23] H. Ikeda, R. Arita, and J. Kuneš, *Phys. Rev. B* **82**, 024508 (2010).
- [24] E. Kaneshita and T. Tohyama, *Phys. Rev. B* **82**, 094441 (2010).
- [25] H. Park, K. Haule, and G. Kotliar, *Phys. Rev. Lett.* **107**, 137007 (2011).
- [26] Z. P. Yin, K. Haule, and G. Kotliar, *Nat. Phys.* **10**, 845 (2014).
- [27] P. Dai, J. Hu, and E. Dagotto, *Nat. Phys.* **8**, 709 (2012).
- [28] J. M. Tranquada, G. Xu, and I. A. Zaliznyak, *Journal of Magnetism and Magnetic Materials* **350**, 148 (2014).
- [29] P. Dai, *Rev. Mod. Phys.* **87**, 855 (2015).
- [30] D. S. Inosov, *C. R. Phys.* **17**, 60 (2016).
- [31] J. Zhao, D.-X. Yao, S. Li, T. Hong, Y. Chen, S. Chang, W. Ratcliff, J. W. Lynn, H. A. Mook, G. F. Chen, J. L. Luo, N. L. Wang, E. W. Carlson, J. Hu, and P. Dai, *Phys. Rev. Lett.* **101**, 167203 (2008).
- [32] R. J. McQueeney, S. O. Diallo, V. P. Antropov, G. D. Samolyuk, C. Broholm, N. Ni, S. Nandi, M. Yethiraj, J. L. Zarestky, J. J. Pulikkotil, A. Kreyssig, M. D. Lumsden, B. N. Harmon, P. C. Canfield, and A. I. Goldman, *Phys. Rev. Lett.* **101**, 227205 (2008).
- [33] A. D. Christianson, E. A. Goremychkin, R. Osborn, S. Rosenkranz, M. D. Lumsden, C. D. Malliakas, I. S. Todorov, H. Claus, D. Y. Chung, M. G. Kanatzidis, R. I. Bewley, and T. Guidi, *Nature* **456**, 930 (2008).
- [34] R. A. Ewings, T. G. Perring, R. I. Bewley, T. Guidi, M. J. Pitcher, D. R. Parker, S. J. Clarke, and A. T. Boothroyd, *Phys. Rev. B* **78**, 220501 (2008).
- [35] M. Ishikado, R. Kajimoto, S.-i. Shamoto, M. Arai, A. Iyo, K. Miyazawa, P. M. Shirage, H. Kito, H. Eisaki, S. Kim, H. Hosono, T. Guidi, R. Bewley, and S. M. Bennington, *J. Phys. Soc. Jpn.* **78**, 043705 (2009).
- [36] A. D. Christianson, M. D. Lumsden, S. E. Nagler, G. J. MacDougall, M. A. McGuire, A. S. Sefat, R. Jin, B. C. Sales, and D. Mandrus, *Phys. Rev. Lett.* **103**, 087002 (2009).
- [37] L. W. Harriger, A. Schneidewind, S. Li, J. Zhao, Z. Li, W. Lu, X. Dong, F. Zhou, Z. Zhao, J. Hu, and P. Dai, *Phys. Rev. Lett.* **103**, 087005 (2009).
- [38] S. O. Diallo, V. P. Antropov, T. G. Perring, C. Broholm, J. J. Pulikkotil, N. Ni, S. L. Bud'ko, P. C. Canfield, A. Kreyssig, A. I. Goldman, and R. J. McQueeney, *Phys. Rev. Lett.* **102**, 187206 (2009).
- [39] J. Zhao, D. T. Adroja, D.-X. Yao, R. Bewley, S. Li, X. F. Wang, G. Wu, X. H. Chen, J. Hu, and P. Dai, *Nat. Phys.* **5**, 555 (2009).
- [40] C. Lester, J.-H. Chu, J. G. Analytis, T. G. Perring, I. R. Fisher, and S. M. Hayden, *Phys. Rev. B* **81**, 064505 (2010).
- [41] D. S. Inosov, J. T. Park, P. Bourges, D. L. Sun, Y. Sidis, A. Schneidewind, K. Hradil, D. Haug, C. T. Lin, B. Keimer, and V. Hinkov, *Nat. Phys.* **6**, 178 (2010).

- [42] S. O. Diallo, D. K. Pratt, R. M. Fernandes, W. Tian, J. L. Zarestky, M. Lumsden, T. G. Perring, C. L. Broholm, N. Ni, S. L. Bud'ko, P. C. Canfield, H.-F. Li, D. Vaknin, A. Kreyssig, A. I. Goldman, and R. J. McQueeney, *Phys. Rev. B* **81**, 214407 (2010).
- [43] D. K. Pratt, A. Kreyssig, S. Nandi, N. Ni, A. Thaler, M. D. Lumsden, W. Tian, J. L. Zarestky, S. L. Bud'ko, P. C. Canfield, A. I. Goldman, and R. J. McQueeney, *Phys. Rev. B* **81**, 140510 (2010).
- [44] M. Wang, H. Luo, J. Zhao, C. Zhang, M. Wang, K. Marty, S. Chi, J. W. Lynn, A. Schneidewind, S. Li, and P. Dai, *Phys. Rev. B* **81**, 174524 (2010).
- [45] J. T. Park, D. S. Inosov, A. Yaresko, S. Graser, D. L. Sun, P. Bourges, Y. Sidis, Y. Li, J.-H. Kim, D. Haug, A. Ivanov, K. Hradil, A. Schneidewind, P. Link, E. Faulhaber, I. Glavatsky, C. T. Lin, B. Keimer, and V. Hinkov, *Phys. Rev. B* **82**, 134503 (2010).
- [46] R. A. Ewings, T. G. Perring, J. Gillett, S. D. Das, S. E. Sebastian, A. E. Taylor, T. Guidi, and A. T. Boothroyd, *Phys. Rev. B* **83**, 214519 (2011).
- [47] C. Zhang, M. Wang, H. Luo, M. Wang, M. Liu, J. Zhao, D. L. Abernathy, T. A. Maier, K. Marty, M. D. Lumsden, S. Chi, S. Chang, J. A. Rodriguez-Rivera, J. W. Lynn, T. Xiang, J. Hu, and P. Dai, *Sci. Rep.* **1**, 115 (2011).
- [48] J.-P. Castellan, S. Rosenkranz, E. A. Goremychkin, D. Y. Chung, I. S. Todorov, M. G. Kanatzidis, I. Eremin, J. Knolle, A. V. Chubukov, S. Maiti, M. R. Norman, F. Weber, H. Claus, T. Guidi, R. I. Bewley, and R. Osborn, *Phys. Rev. Lett.* **107**, 177003 (2011).
- [49] L. W. Harriger, H. Q. Luo, M. S. Liu, C. Frost, J. P. Hu, M. R. Norman, and P. Dai, *Phys. Rev. B* **84**, 054544 (2011).
- [50] M. Liu, L. W. Harriger, H. Luo, M. Wang, R. A. Ewings, T. Guidi, H. Park, K. Haule, G. Kotliar, S. M. Hayden, and P. Dai, *Nat. Phys.* **8**, 376 (2012).
- [51] G. S. Tucker, R. M. Fernandes, H.-F. Li, V. Thampy, N. Ni, D. L. Abernathy, S. L. Bud'ko, P. C. Canfield, D. Vaknin, J. Schmalian, and R. J. McQueeney, *Phys. Rev. B* **86**, 024505 (2012).
- [52] H. Luo, Z. Yamani, Y. Chen, X. Lu, M. Wang, S. Li, T. A. Maier, S. Danilkin, D. T. Adroja, and P. Dai, *Phys. Rev. B* **86**, 024508 (2012).
- [53] L. W. Harriger, M. Liu, H. Luo, R. A. Ewings, C. D. Frost, T. G. Perring, and P. Dai, *Phys. Rev. B* **86**, 140403 (2012).
- [54] S. Iimura, S. Matsuishi, M. Miyakawa, T. Taniguchi, K. Suzuki, H. Usui, K. Kuroki, R. Kajimoto, M. Nakamura, Y. Inamura, K. Ikeuchi, S. Ji, and H. Hosono, *Phys. Rev. B* **88**, 060501 (2013).
- [55] H. Luo, X. Lu, R. Zhang, M. Wang, E. A. Goremychkin, D. T. Adroja, S. Danilkin, G. Deng, Z. Yamani, and P. Dai, *Phys. Rev. B* **88**, 144516 (2013).
- [56] M. Wang, C. Zhang, X. Lu, G. Tan, H. Luo, Y. Song, M. Wang, X. Zhang, E. A. Goremychkin, T. G. Perring, T. A. Maier, Z. Yin, K. Haule, G. Kotliar, and P. Dai, *Nat. Commun.* **4**, 2874 (2013).
- [57] G. S. Tucker, R. M. Fernandes, D. K. Pratt, A. Thaler, N. Ni, K. Marty, A. D. Christianson, M. D. Lumsden, B. C. Sales, A. S. Sefat, S. L. Bud'ko, P. C. Canfield, A. Kreyssig, A. I. Goldman, and R. J. McQueeney, *Phys. Rev. B* **89**, 180503 (2014).
- [58] C. Zhang, L. W. Harriger, Z. Yin, W. Lv, M. Wang, G. Tan, Y. Song, D. L. Abernathy, W. Tian, T. Egami, K. Haule, G. Kotliar, and P. Dai, *Phys. Rev. Lett.* **112**, 217202 (2014).
- [59] X. Lu, J. T. Park, R. Zhang, H. Luo, A. H. Nevidomskyy, Q. Si, and P. Dai, *Science* **345**, 657 (2014).
- [60] N. Qureshi, P. Steffens, D. Lamago, Y. Sidis, O. Sobolev, R. A. Ewings, L. Harnagea, S. Wurmehl, B. Büchner, and M. Braden, *Phys. Rev. B* **90**, 144503 (2014).
- [61] M. C. Rahn, R. A. Ewings, S. J. Sedlmaier, S. J. Clarke, and A. T. Boothroyd, *Phys. Rev. B* **91**, 180501 (2015).
- [62] Y. Song, X. Lu, D. L. Abernathy, D. W. Tam, J. L. Niedziela, W. Tian, H. Luo, Q. Si, and P. Dai, *Phys. Rev. B* **92**, 180504 (2015).
- [63] M. G. Kim, M. Wang, G. S. Tucker, P. N. Valdivia, D. L. Abernathy, S. Chi, A. D. Christianson, A. A. Aczel, T. Hong, T. W. Heitmann, S. Ran, P. C. Canfield, E. D. Bourret-Courchesne, A. Kreyssig, D. H. Lee, A. I. Goldman, R. J. McQueeney, and R. J. Birgeneau, *Phys. Rev. B* **92**, 214404 (2015).
- [64] Q. Wang, Y. Shen, B. Pan, Y. Hao, M. Ma, F. Zhou, P. Steffens, K. Schmalzl, T. R. Forrest, M. Abdel-Hafez, X. Chen, D. A. Chareev, A. N. Vasiliev, P. Bourges, Y. Sidis, H. Cao, and J. Zhao, *Nat. Mater.* **15**, 159 (2016).
- [65] Y. Li, Z. Yin, X. Wang, D. W. Tam, D. L. Abernathy, A. Podlesnyak, C. Zhang, M. Wang, L. Xing, C. Jin, K. Haule, G. Kotliar, T. A. Maier, and P. Dai, *Phys. Rev. Lett.* **116**, 247001 (2016).
- [66] Q. Wang, Y. Shen, B. Pan, X. Zhang, K. Ikeuchi, K. Iida, A. D. Christianson, H. C. Walker, D. T. Adroja, M. Abdel-Hafez, X. Chen, D. A. Chareev, A. N. Vasiliev, and J. Zhao, *Nat. Commun.* **7**, 12182 (2016).
- [67] D. Hu, Z. Yin, W. Zhang, R. A. Ewings, K. Ikeuchi, M. Nakamura, B. Roessli, Y. Wei, L. Zhao, G. Chen, S. Li, H. Luo, K. Haule, G. Kotliar, and P. Dai, *Phys. Rev. B* **94**, 094504 (2016).
- [68] T. Xie, D. Gong, H. Ghosh, A. Ghosh, M. Soda, T. Masuda, S. Itoh, F. Bourdarot, L.-P. Regnault, S. Danilkin, S. Li, and H. Luo, *Phys. Rev. Lett.* **120**, 137001 (2018).
- [69] A. Sapkota, P. Das, A. E. Böhrer, B. G. Ueland, D. L. Abernathy, S. L. Bud'ko, P. C. Canfield, A. Kreyssig, A. I. Goldman, and R. J. McQueeney, *Phys. Rev. B* **97**, 174519 (2018).
- [70] N. Murai, K. Suzuki, S.-i. Ideta, M. Nakajima, K. Tanaka, H. Ikeda, and R. Kajimoto, *Phys. Rev. B* **97**, 241112 (2018).
- [71] X. Lu, D. D. Scherer, D. W. Tam, W. Zhang, R. Zhang, H. Luo, L. W. Harriger, H. C. Walker, D. T. Adroja, B. M. Andersen, and P. Dai, *Phys. Rev. Lett.* **121**, 067002 (2018).
- [72] J. Guo, L. Yue, K. Iida, K. Kamazawa, L. Chen, T. Han, Y. Zhang, and Y. Li, *Phys. Rev. Lett.* **122**, 017001 (2019).
- [73] T. Chen, Y. Chen, A. Kreisel, X. Lu, A. Schneidewind, Y. Qiu, J. T. Park, T. G. Perring, J. R. Stewart, H. Cao, R. Zhang, Y. Li, Y. Rong, Y. Wei, B. M. Andersen, P. J. Hirschfeld, C. Broholm, and P. Dai, *Nat. Mater.* **18**, 709 (2019).
- [74] F. Waßer, J. T. Park, S. Aswartham, S. Wurmehl, Y. Sidis, P. Steffens, K. Schmalzl, B. Büchner, and M. Braden, *npj Quantum Materials* **4**, 59 (2019).
- [75] S. Shen, X. Zhang, H. Wo, Y. Shen, Y. Feng, A. Schneidewind, P. Čermák, W. Wang, and J. Zhao, *Phys. Rev.*

- Lett.* **124**, 017001 (2020).
- [76] M. Nakajima, M. Nagafuchi, and S. Tajima, *Phys. Rev. B* **97**, 094511 (2018).
- [77] R. Kajimoto, M. Nakamura, Y. Inamura, F. Mizuno, K. Nakajima, S. Ohira-Kawamura, T. Yokoo, T. Nakatani, R. Maruyama, K. Soyama, K. Shibata, K. Suzuya, S. Sato, K. Aizawa, M. Arai, S. Wakimoto, M. Ishikado, S.-i. Shamoto, M. Fujita, H. Hiraka, K. Ohoyama, K. Yamada, and C.-H. Lee, *J. Phys. Soc. Jpn.* **80**, SB025 (2011).
- [78] M. Nakamura, R. Kajimoto, Y. Inamura, F. Mizuno, M. Fujita, T. Yokoo, and M. Arai, *J. Phys. Soc. Jpn.* **78**, 093002 (2009).
- [79] K. Nakajima, S. Ohira-Kawamura, T. Kikuchi, M. Nakamura, R. Kajimoto, Y. Inamura, N. Takahashi, K. Aizawa, K. Suzuya, K. Shibata, T. Nakatani, K. Soyama, R. Maruyama, H. Tanaka, W. Kambara, T. Iwahashi, Y. Itoh, T. Osakabe, S. Wakimoto, K. Kakurai, F. Maekawa, M. Harada, K. Oikawa, R. E. Lechner, F. Mezei, and M. Arai, *J. Phys. Soc. Jpn.* **80**, SB028 (2011).
- [80] Y. Inamura, T. Nakatani, J. Suzuki, and T. Otomo, *J. Phys. Soc. Jpn.* **82**, SA031 (2013).
- [81] Y. Inamura, [Utsusemi Portal Site](#).
- [82] P. Giannozzi, S. Baroni, N. Bonini, M. Calandra, R. Car, C. Cavazzoni, D. Ceresoli, G. L. Chiarotti, M. Cococcioni, I. Dabo, A. D. Corso, S. de Gironcoli, S. Fabris, G. Fratesi, R. Gebauer, U. Gerstmann, C. Gougoussis, A. Kokalj, M. Lazzeri, L. Martin-Samos, N. Marzari, F. Mauri, R. Mazzarello, S. Paolini, A. Pasquarello, L. Paulatto, C. Sbraccia, S. Scandolo, G. Sclauzero, A. P. Seitsonen, A. Smogunov, P. Umari, and R. M. Wentzcovitch, *J. Phys. Condens. Matter* **21**, 395502 (2009).
- [83] P. Giannozzi, O. Andreussi, T. Brumme, O. Bunau, M. B. Nardelli, M. Calandra, R. Car, C. Cavazzoni, D. Ceresoli, M. Cococcioni, N. Colonna, I. Carnimeo, A. D. Corso, S. de Gironcoli, P. Delugas, R. A. DiStasio, A. Ferretti, A. Floris, G. Fratesi, G. Fugallo, R. Gebauer, U. Gerstmann, F. Giustino, T. Gorni, J. Jia, M. Kawamura, H.-Y. Ko, A. Kokalj, E. Küçükbenli, M. Lazzeri, M. Marsili, N. Marzari, F. Mauri, N. L. Nguyen, H.-V. Nguyen, A. O. de-la Roza, L. Paulatto, S. Poncé, D. Rocca, R. Sabatini, B. Santra, M. Schlipf, A. P. Seitsonen, A. Smogunov, I. Timrov, T. Thonhauser, P. Umari, N. Vast, X. Wu, and S. Baroni, *J. Phys. Condens. Matter* **29**, 465901 (2017).
- [84] A. A. Mostofi, J. R. Yates, Y.-S. Lee, I. Souza, D. Vanderbilt, and N. Marzari, *Comput. Phys. Commun.* **178**, 685 (2008).
- [85] G. Pizzi, V. Vitale, R. Arita, S. Blügel, F. Freimuth, G. Géranton, M. Gibertini, D. Gresch, C. Johnson, T. Koretsune, J. Ibañez-Azpiroz, H. Lee, J.-M. Lihm, D. Marchand, A. Marrazzo, Y. Mokrousov, J. I. Mustafa, Y. Nohara, Y. Nomura, L. Paulatto, S. Poncé, T. Ponweiser, J. Qiao, F. Thöle, S. S. Tsirkin, M. Wierzbowska, N. Marzari, D. Vanderbilt, I. Souza, A. A. Mostofi, and J. R. Yates, *J. Phys. Condens. Matter* **32**, 165902 (2020).
- [86] J. P. Perdew, K. Burke, and M. Ernzerhof, *Phys. Rev. Lett.* **77**, 3865 (1996).
- [87] C. Liu, G. D. Samolyuk, Y. Lee, N. Ni, T. Kondo, A. F. Santander-Syro, S. L. Bud'ko, J. L. McChesney, E. Rotenberg, T. Valla, A. V. Fedorov, P. C. Canfield, B. N. Harmon, and A. Kaminski, *Phys. Rev. Lett.* **101**, 177005 (2008).
- [88] K. Yada and H. Kontani, *J. Phys. Soc. Jpn.* **74**, 2161 (2005).
- [89] The doping effect is modeled through a rigid band shift of the Fermi level. To follow the convention often used in prior studies, the Fermi surfaces in Figs. 1(a)-(c) are shown in the folded BZ for the crystallographic unit cell (2-Fe/unit cell). For the RPA calculations, however, we used an effective five-orbital model in the unfolded BZ of the 1-Fe/unit cell, which better reflects the symmetry of spin susceptibility in FeSCs.
- [90] P. Vilmercati, A. Fedorov, I. Vobornik, U. Manju, G. Panaccione, A. Goldoni, A. S. Sefat, M. A. McGuire, B. C. Sales, R. Jin, D. Mandrus, D. J. Singh, and N. Mannella, *Phys. Rev. B* **79**, 220503 (2009).
- [91] W. Malaeb, T. Yoshida, A. Fujimori, M. Kubota, K. Ono, K. Kihou, P. M. Shirage, H. Kito, A. Iyo, H. Eisaki, Y. Nakajima, T. Tamegai, and R. Arita, *J. Phys. Soc. Jpn.* **78**, 123706 (2009).
- [92] T. Yoshida, I. Nishi, S. Ideta, A. Fujimori, M. Kubota, K. Ono, S. Kasahara, T. Shibauchi, T. Terashima, Y. Matsuda, H. Ikeda, and R. Arita, *Phys. Rev. Lett.* **106**, 117001 (2011).
- [93] V. Brouet, M. F. Jensen, P.-H. Lin, A. Taleb-Ibrahimi, P. Le Fèvre, F. Bertran, C.-H. Lin, W. Ku, A. Forget, and D. Colson, *Phys. Rev. B* **86**, 075123 (2012).
- [94] S. Ideta, T. Yoshida, I. Nishi, A. Fujimori, Y. Kotani, K. Ono, Y. Nakashima, S. Yamaichi, T. Sasagawa, M. Nakajima, K. Kihou, Y. Tomioka, C. H. Lee, A. Iyo, H. Eisaki, T. Ito, S. Uchida, and R. Arita, *Phys. Rev. Lett.* **110**, 107007 (2013).
- [95] Z. R. Ye, Y. Zhang, F. Chen, M. Xu, Q. Q. Ge, J. Jiang, B. P. Xie, and D. L. Feng, *Phys. Rev. B* **86**, 035136 (2012).
- [96] H. Suzuki, T. Kobayashi, S. Miyasaka, T. Yoshida, K. Okazaki, L. C. C. Ambolode, S. Ideta, M. Yi, M. Hashimoto, D. H. Lu, Z.-X. Shen, K. Ono, H. Kumigashira, S. Tajima, and A. Fujimori, *Phys. Rev. B* **89**, 184513 (2014).
- [97] S. Ideta, N. Murai, M. Nakajima, R. Kajimoto, and K. Tanaka, *Phys. Rev. B* **100**, 235135 (2019).
- [98] M. Arai, in *Neutron Scattering - Fundamentals*, edited by F. Fernandez-Alonso and D. L. Price (Academic Press, 2013) Chap. 3, pp. 245-320.
- [99] A. T. Boothroyd, *Principles of Neutron Scattering from Condensed Matter* (Oxford University Press, 2020).
- [100] M. D. Watson, T. K. Kim, A. A. Haghighirad, N. R. Davies, A. McCollam, A. Narayanan, S. F. Blake, Y. L. Chen, S. Ghannadzadeh, A. J. Schofield, M. Hoesch, C. Meingast, T. Wolf, and A. I. Coldea, *Phys. Rev. B* **91**, 155106 (2015).
- [101] M. D. Watson, S. Backes, A. A. Haghighirad, M. Hoesch, T. K. Kim, A. I. Coldea, and R. Valentí, *Phys. Rev. B* **95**, 081106 (2017).
- [102] X. Long, S. Zhang, F. Wang, and Z. Liu, *npj Quantum Mater.* **5**, 50 (2020).
- [103] T. Yamada and T. Tohyama, *Phys. Rev. B* **104**, L161110 (2021).
- [104] M. Aichhorn, S. Biermann, T. Miyake, A. Georges, and M. Imada, *Phys. Rev. B* **82**, 064504 (2010).
- [105] S. Mandal, P. Zhang, S. Ismail-Beigi, and K. Haule, *Phys. Rev. Lett.* **119**, 067004 (2017).

- [106] S. Acharya, D. Pashov, and M. van Schilfgaarde, *Phys. Rev. B* **105**, 144507 (2022).
- [107] M. Ma, P. Bourges, Y. Sidis, J. Sun, G. Wang, K. Iida, K. Kamazawa, J. T. Park, F. Bourdarot, Z. Ren, and Y. Li, *Phys. Rev. B* **110**, 174503 (2024).